ELSEVIER

Journal of Nuclear Materials 290–293 (2001) 525–529

journal of nuclear materials

www.elsevier.nl/locate/jnucmat

Radiation distribution and power balance in the ASDEX Upgrade LYRA divertor

J.C. Fuchs *, D. Coster, A. Herrmann, A. Kallenbach, K.F. Mast, ASDEX Upgrade Team

Max-Planck-Institut für Plasmaphysik, EURATOM Association, Boltzmannstrasse 2, D-85748 Garching, Germany

Abstract

Radiation distribution and heat load on the target plates of ASDEX Upgrade are investigated over a wide experimental parameter range with discharges up to 20 MW heating power and $\bar{n}_e = (0.4–0.8)n_{GW}$. Integrating the radiation density over the whole plasma yields a total radiated power of about 80% of the input power, and radiation from the divertor and *X*-point region is about 40% of the input power. Whereas the radiated power in the main plasma is comparable for the former open divertor I (Div I) and the new closed LYRA divertor (Div II), the radiation fraction in the divertor has nearly doubled for the LYRA divertor. Simultaneous to the increased divertor radiation in the LYRA divertor, the maximum heat flux density to the target plates, measured by thermographic cameras, is reduced by a factor of about two compared to that in Div I for comparable attached conditions. Furthermore, especially in the inner divertor fan, the radiation contributes to a large part of the measured heat flux.

Keywords: ASDEX-Upgrade; Radiation loss; Divertor; Heat flux

1. Introduction

Radiation losses in the new closed Lyra divertor (Div II) of ASDEX Upgrade are investigated. A detailed knowledge of the radiation distribution in the divertor is necessary in order to increase and control the divertor radiation with the aim of reducing the power load on the divertor plates under ITER relevant conditions.

In ASDEX Upgrade, radiation losses are measured with 100 bolometers placed in seven pinhole cameras which are mounted in one poloidal cross-section of the torus inside the vacuum vessel. Two bolometer pinhole cameras each with seven lines of sight measure radiation from the inner and outer divertor legs and allow for a correction of the neutral gas pressure dependent bolometer sensitivity and of the residual bolometer offset drift. The region around the *X*-point is observed with an eight channel pinhole camera, the main plasma with 72 bolometers placed in five cameras. The bolometers are miniaturized, low noise metal resistor bolometers [1] which are excited by a 50 kHz sine wave and effectively suppress thermal drift and electromagnetic interferences.

In order to obtain the distribution of the local radiation emissivity in a poloidal cross-section of the plasma, the measured line integrals must be unfolded. This is done with the 'Anisotropic Diffusion Model Tomography' algorithm, which is based on the fact that the variation of the radiation emissivity along magnetic field lines is much smaller than perpendicular to them. This behavior is described by an anisotropic diffusion model with different values of the diffusion coefficients $D_\perp$, $D_\parallel$ along and perpendicular to the magnetic field lines [2].

2. Radiation pattern

The measured line integrals of the 22 divertor bolometers together with the other 72 bolometers of ASDEX Upgrade have been unfolded in order to reconstruct the radiation distribution in the divertor region as well as in the main chamber.

* Corresponding author. Tel.: +49-89 3299 1730; fax: +49-89 3299 2580.

E-mail address: christoph.fuchs@ipp.mpg.de (J.C. Fuchs).

0022-3115/01/$ - see front matter
PII: S0022-3115(00)00645-0

2.1. Radiation distribution

Fig. 1 shows a typical, ELM-averaged radiation profile for a discharge with $I_p = 1$ MA, $\overline{n_e} = 7 \times 10^{19}$ m^{-3}, $q_{95} = 4$ and 15 MW neutral beam injection power. The highest radiation is found in the divertor fans near the strike points with local radiation emissivities of up to 30 MW m^{-3} at the inner and 12 MW m^{-3} at the outer strike point. The radiation in the inner divertor is higher than in the outer divertor due to ELMs.

A reconstruction of the radiation distribution between ELMs is possible for low frequency ELMs. In this case, the distribution is more symmetric between inner and outer divertor fan, and the maximum emissivities are much smaller (about half) than for the ELM-averaged profiles in the inner divertor (Fig. 3).

There is also radiation between the strike points and the X-point, which will be discussed later more in detail. In the main plasma, one finds radiation mainly along the separatrix with emissivities of few MW m^{-3}. The shape of the radiation profile does not change considerably if the neutral beam injection power is increased, but scales almost linearly with the heating power.

Integrating the radiation emissivity over the whole plasma, one finds that the total radiated power is about 60–80% of the input power (Fig. 2). Radiation from the divertor and X-point region (defined by a horizontal line through the X-point) is about 40–50% of the input power, which is clearly higher than the radiated fraction in Div I, thus also reducing the power load onto the divertor plates [5]. Also these values are almost independent of the heating power (Fig. 4) [3,4].

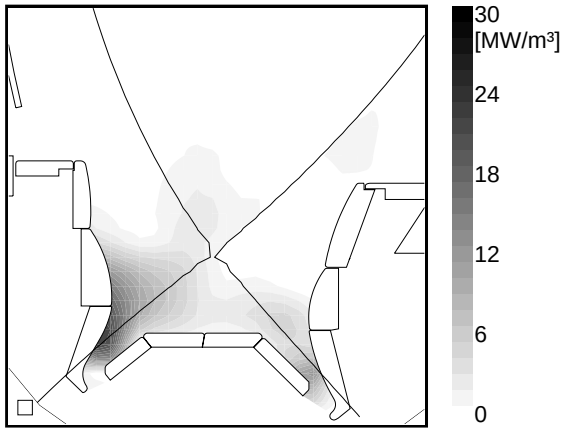

Fig. 1. Reconstructed ELM-averaged radiation pattern in the ASDEX Upgrade LYRA divertor with pronounced radiation peaks in the inner and outer divertor fan for an H-mode discharge with 15 MW input power.

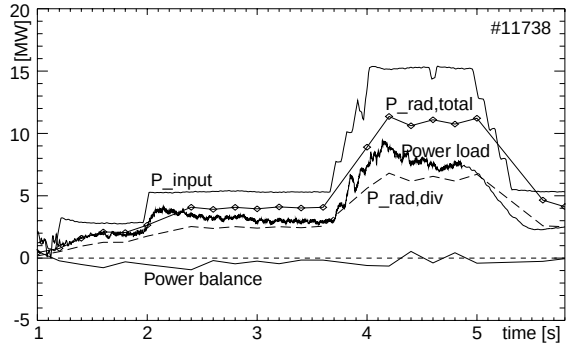

Fig. 2. Radiated power and power balance for the discharge from Fig. 1, showing time traces of the input power, the total radiated power, radiated power in the divertor, power load on the divertor plates measured by thermographic cameras and the radiation corrected power balance.

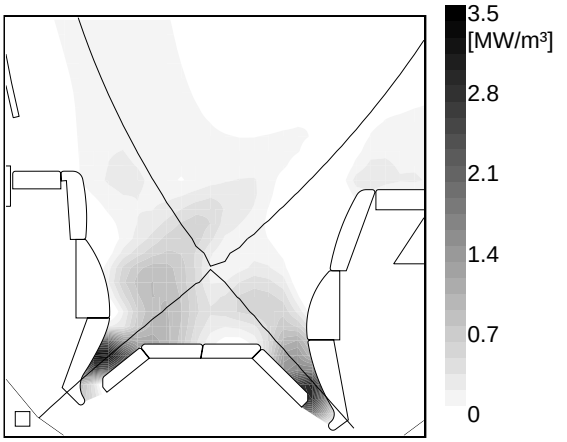

Fig. 3. Reconstructed radiation distribution between low frequency ELMs for an H-mode discharge with 2.5 MW input power.

2.2. Radiation band

Modeling of the radiation emissivity with the B2-Eirene code predicts a small radiation zone along the separatrix between the strike points and the X-point (Fig. 5(a)) [6], however due to the limited spatial resolution of the bolometer lines of sight, these radiation bands cannot be detected in normal plasma discharges. Therefore, the plasma was shifted vertically for about 10 cm, such that the region of interest was moved over several channels of the bolometer cameras. From the time evolution of the measured line integrals during the plasma shift, several 'virtual lines of sight' were constructed and used for the reconstruction of the radiation pattern. Fig. 5(b) shows the result for a discharge with 5 MW neutral beam injection power ($I_p = 1$ MA, $\overline{n_e} = 5.4 \times 10^{19}$ m^{-3}, $B_T = -2.5$ T). The predicted radiation band is clearly

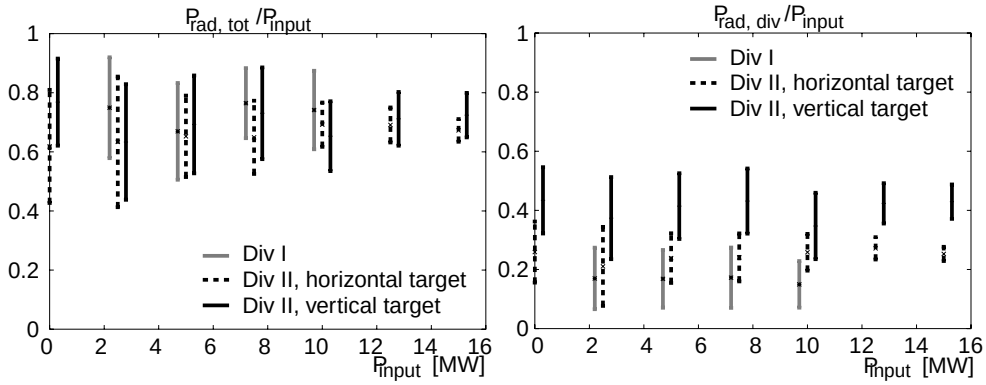

Fig. 4. Fraction of the total radiated power to the input power (left) and the radiated power in the divertor to the input power (right) as a function of the input power. Solid black: outer strike point on the strike point-module (vertical target), dashed black: outer strike point on the roof baffle (horizontal target), gray: Div I (two horizontal targets). The lines indicate the standard deviation for a large

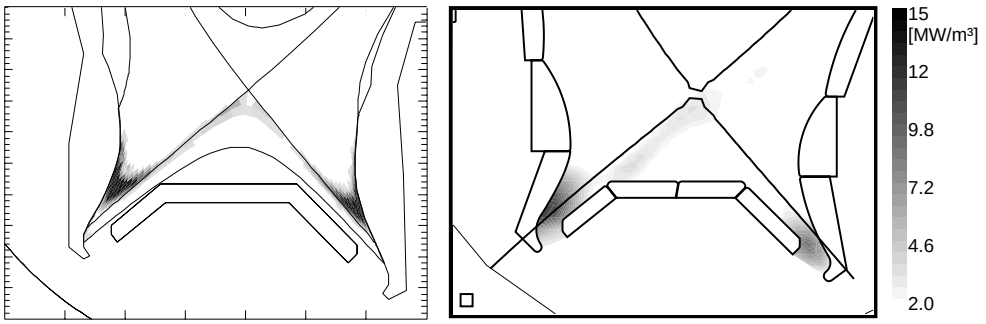

Fig. 5. Left: B2-Eirene modeling of the radiation distribution, right: the reconstructed radiation distribution using virtual lines of sight shows a narrow radiation zone from the strike point to the *X*-point.

seen with a width of few centimeters and an emissivity of ca 3–4 MW m^{-3} at the inner divertor. (Since there are no suitable lines of sight at the outer divertor yet, the corresponding band there cannot be detected.)

Measurements from various spectrometers as well as modeling with B2-Eirene show that the radiation directly above the strike points origins from hydrogen and carbon (CII), and the radiation band consists mainly of carbon radiation, where CII, CIII, and CIV follow from the strike point to the *X*-point.

2.3. Comparison with Divertor I

Fig. 6 shows a comparison of the radiation distribution in the former open Div I and the new closed Div II of ASDEX Upgrade for two similar L-mode discharges ($P_{NI} = 2.5$ MW, $I_p = 0.8$ MA, $\overline{n_e} = 5 \times 10^{19}$ m^{-3}). In Div II, there is more radiation than in Div I, and it is more concentrated in the divertor fans. Also the radiation distribution in the divertor fans of Div II is more symmetric than over the target plates of Div I.

Whereas the radiation losses in the main plasma are comparable for both divertor configurations, we find that the radiation from the LYRA divertor is twice as high as the radiation from the Div I (Fig. 4).

2.4. Horizontal and vertical target plates

For discharges with increased triangularity in the present divertor configuration, the outer strike point must be moved on the roof baffle, which means a horizontal target plate and a more open divertor in contrast to the normal vertical and closed one. Fig. 7 shows the radiation profile for such a discharge with a horizontal target plate and $I_p = 1$ MA , $\overline{n_e} = 13 \times 10^{19}$ m^{-3}, $q_{95} = 4$ and 13 MW neutral beam injection power. Again we find the highest radiation near the strike points, however at the outer strike point, the radiation density now is about 15 MW m^{-3}. Whereas the total radiated power (75% of the input power) remains nearly unchanged compared to discharges with both strike points on the vertical plates, the divertor radiation is lower (only 25%

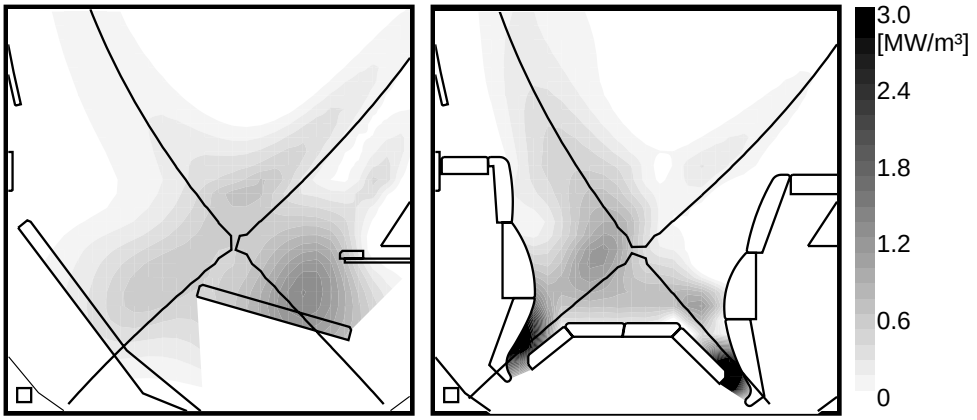

Fig. 6. Comparison of the radiation distribution for Div I (left) and Div II (right) for comparable conditions (2.5 MW input power, L-mode).

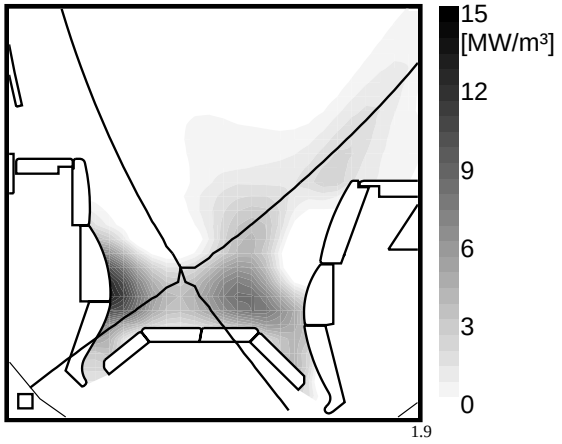

Fig. 7. Radiation profile for a shot with the outer strike point on roof baffle (horizontal target). The input power is 15 MW.

of the input power), and the radiation in the main chamber has increased. Also these values are nearly independent of the heating power (Fig. 4), and they are comparable to the values from the former Div I of ASDEX Upgrade, where both strike points were on almost horizontal target plates [5].

3. Power balance

Summing up the input power, the total radiated power measured by bolometers, the power load on the divertor plates measured by IR-cameras, and the change in the MHD energy of the plasma, one arrives typically for all types of discharges (ohmic, L-, and H-mode) at a larger value than the input power (Fig. 2). However, parts of the divertor radiation are measured by both bolometer and IR-cameras. From the reconstructed radiation profile, one can calculate the radiated power onto the divertor plates. Correcting the power balance by this value, one arrives at a reasonably good power balance within 20% error bars.

Comparing the power density on the divertor plates measured by thermography with the radiation density on the plates calculated from the reconstructed radiation profiles, one finds that in the inner divertor, a large part of the power load origins due to radiation. In contrast to the conductive/convective heat flux, the radiative heat flux is loaded on a wide divertor region with a maximum load well below 1 MW m^{-2}. In the outer divertor, however, radiation is only a small part of the power load on the divertor plates (Fig. 8).

4. Summary and conclusions

The radiation distribution in the closed ASDEX Upgrade LYRA divertor normally shows two pronounced peaks of the radiation density in both the inner and outer divertor near the strike points, which may be higher than 30 MW m^{-3} in discharges with 15 MW heating power. Integrating the radiation density over the whole plasma yields a total radiated power of about 70–80% of the input power, this fraction is almost independent of the input power. Radiation from the divertor and the X-point region is about 40–50% of the input power, also this fraction is nearly independent of the the input power.

The measured and reconstructed radiation distribution is also reproduced in detail by the B2-Eirene code, if the carbon sputtering yield and the perpendicular transport coefficients are properly adopted. This code also shows in accordance with the spectrometric measurements that the radiation is mostly carbon and hydrogen radiation.

Radiation losses in the ASDEX Upgrade divertor are found to be higher than that in other machines like JET

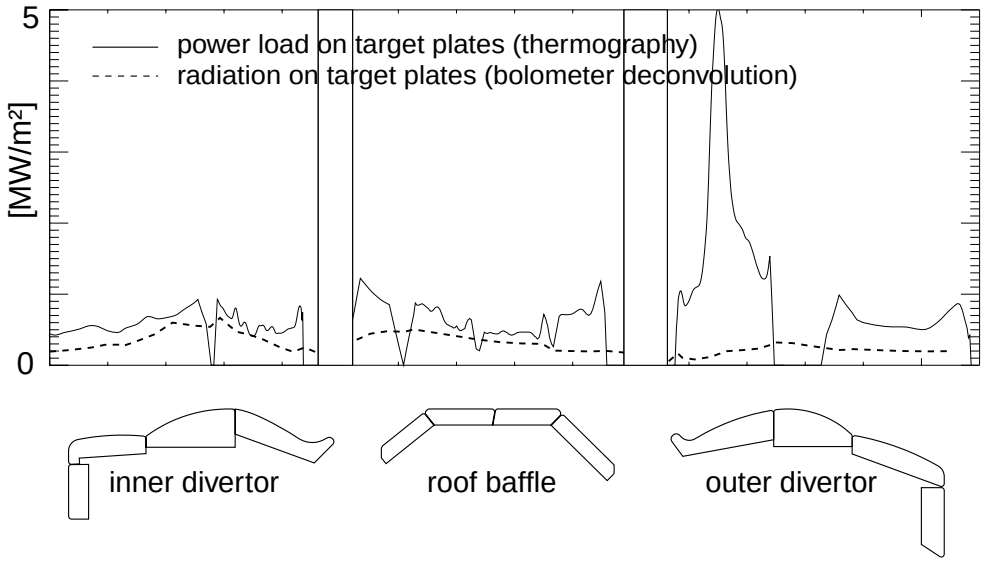

Fig. 8. Power load on divertor plates measured by thermography (solid line) and radiation on plates calculated from the reconstructed profile (dashed line) for the 15 MW discharge from Fig. 1 (ELM averaged).

[7] and to some degree DIII-D [8]. The higher radiation in ASDEX Upgrade compared to JET is correlated to a higher edge electron density and lower electron temperature in the divertor, so that carbon radiates more effectively. The origin of these differences however is still subject to further studies.

Whereas radiation losses in the main plasma are comparable for the former open Div I and the new closed LYRA divertor, the radiation fraction in the divertor has nearly doubled for the LYRA divertor, where both strike points are on vertical target plates instead of horizontal ones. However, if in the LYRA divertor the outer strike point is moved to a horizontal target, which also means a more open divertor, the divertor radiation decreases to about 25–30% of the input power.

Simultaneously to the increased divertor radiation in the LYRA divertor, the maximum heat flux density to the target plates, measured by thermographic cameras, is reduced by a factor of about two compared to that in Div I for comparable attached conditions. Furthermore, especially in the inner divertor fan, the radiation contributes to a large part of the measured heat flux, and is loaded over a wide divertor region in contrast to the conductive/convective heat flux.

Modeling of the radiation density with the B2-EIRENE code predicts small radiation zones between the strike points and the *X*-point, which are too small to be detected by the bolometer lines of sight. The existence of this radiation band could be proved by shifting the plasma vertically and increasing the space resolution of the bolometers. Measurements with various spectrometers as well as modelings show that the radiation directly above the strike points origin from hydrogen and carbon (C II, C III, C IV), whereas the radiation band consists of carbon radiation (C III, C IV).

The total power balance for ohmic, L- and H-mode discharges, considering input power, radiation measured by bolometers, power load on the divertor plates measured by thermography, and change of the MHD energy tends to be over-compensated, however taking into account that parts of the divertor radiation are measured by both bolometer and thermographic cameras, one normally arrives at a reasonably good power balance for the LYRA divertor.

These results show, that a closed divertor is more favorable in order to reduce the power load on the target plates.

References

[1] K.F. Mast, J.C. Vallet, C. Andelfinger et al., Rev. Sci. Instr. 63 (3) (1991) 744.
[2] J.C. Fuchs, K.F. Mast, A. Herrmann, K. Lackner, Contribution 21st EPS (1994) 1308ff.
[3] A. Kallenbach, M. Kaufmann, D. Coster, J.C. Fuchs et al., Nucl. Fus. 39 (1999) 901ff.
[4] J.C. Fuchs, K.F. Mast, D. Coster, A. Herrmann, R. Schneider, Contribution 26th EPS (1999) 1385ff.
[5] A. Herrmann, J.C. Fuchs, V. Rohde, M. Weinlich et al., J. Nucl. Mater. 266–269 (1999) 291–295.
[6] D.P. Coster, R. Schneider, H.S. Bosch, A. Carlson, J.C. Fuchs et al., Czech. J. Phys. 48 (Suppl. S2) (1998) 327ff.
[7] A. Loarte et al., Nucl. Fus. 38 (1998) 331.
[8] C. Lasnier et al., Nucl. Fus. 38 (1998) 1225.